Catalysis Today 141 (2009) 72–76

Contents lists available at ScienceDirect

Catalysis Today

journal homepage: www.elsevier.com/locate/cattod

Copper-based catalysts for water gas shift reaction: Influence of support on their catalytic activity

S. Pradhan, A. Satyanarayana Reddy, R.N. Devi, Satyanarayana Chilukuri *

Catalysis and Inorganic Chemistry Division, National Chemical Laboratory, Dr. Homi Bhaba Road, Pune 411008, India

ARTICLE INFO

Article history:
Available online 15 August 2008

Keywords:
Water gas shift
Copper
Ceria
Ceria-zirconia
Ceria-titania
Co-precipitation

ABSTRACT

Three copper containing catalysts supported on ceria and mixed oxides of ceria with zirconia and titania were prepared by co-precipitation method and their catalytic activity was tested for water gas shift (WGS) reaction. High surface area (>100 m^2/g) mixed oxides were obtained following the present method of preparation. The catalysts were characterized by XRD, H_2-temperature programmed reduction (TPR), UV–vis and XPS. Catalytic activity was evaluated for water gas shift reaction in the 200–400 °C temperature range. The gas hourly space velocity was varied from 5000 to 25,000 h^{-1} for better evaluation and comparison of their performance. The effect of CO_2 in the feed gas mixture on the WGS activity of these catalysts was also studied. Among the three catalysts studied, CuO-CeO_2-ZrO_2 mixed oxide shows better activity, implying the influence of support. Characterization of the catalysts after WGS reaction was also carried out in order to investigate structure–property correlation.

1. Introduction

Polymer electrolyte membrane (PEM) fuel cells are expected to play crucial role in the future success of hydrogen economy [1–5]. Currently, hydrogen generation is carried out in large-scale stationary units, either through steam reforming or autothermal reforming of hydrocarbons [6], particularly natural gas or naphtha. However, there is hardly any distribution and storage network to supply the hydrogen for distributed production of back-up electric power using the more efficient fuel cells. Hence, there is a need to generate hydrogen locally in a distributed way, so that it can be fed to PEM fuel cells. The reformate gas that comes out of a steam or autothermal reformer mostly contains a very high content of carbon monoxide, which varies in the range 8–15 vol.% depending on the operating conditions. These hydrogen rich feeds containing high concentration of CO cannot be directly used by PEMFC as CO can poison the Pt anode catalyst, through irreversible adsorption at low temperatures of operation. Hence, similar to present industrial practice, CO content has to be brought down by reacting it with water in presence of an active catalyst, called water gas shift (WGS) reaction. This step while reducing the CO content, enriches the hydrogen in the reformate [7,8]. Followed by this step, pure hydrogen is produced by pressure swing adsorption. Alternately, a preferential oxidation step helps to remove the low content of CO to trace levels in the gas stream to make it eligible as fuel for PEM fuel cells.

The WGS is usually carried out in two stages, a high temperature shift (HTS) carried out in 350–400 °C zone to bring CO in the range of 2–3 vol.% followed by low temperature shift (LTS) carried out in the 180–200 °C temperature zone to bring down the CO to very low levels up to 0.3 vol.% [9,10]. The WGS reaction, which converts CO to $H_2 + CO_2$ by reaction with water, is exothermic as given below:

$$CO + H_2O \Leftrightarrow H_2 + CO_2; \quad \Delta H = -41.1\ \text{kJ/mole}$$

Since, the WGS reaction is thermodynamic equilibrium controlled; it is favoured at low temperatures. On the other hand, kinetically, the catalysts are not so active to attain the equilibrium at low temperatures. Commercial high temperature (350–400 °C) shift reactors contain Fe_2O_3-Cr_2O_3 oxide-based catalysts while LTS is usually a mixed oxide of CuO-ZnO-Al_2O_3, active at lower temperatures (180–200 °C) [11]. Both the catalysts can handle very low space velocities in the range of 2000–4000 h^{-1}, depending on the inlet CO content. Moreover, the HTS catalyst has to be operated carefully to avoid formation of Cr(VI), while the LTS catalysts have limited use in small scale and mobile applications as they are extremely pyrophoric upon exposure to air during the frequent shut-off and switch-on procedures involved in such cases [12]. Hence, there is a need for developing a non-pyrophoric and stable catalyst that can give required activity at high space velocities,

* Corresponding author. Tel.: +91 20 25902019; fax: +91 20 25902633.
E-mail address: sv.chilukuri@ncl.res.in (S. Chilukuri).

0920-5861/$ – see front matter © 2008 Elsevier B.V. All rights reserved.
doi:10.1016/j.cattod.2008.06.026

leading to compact shift reactors. Additionally, instead of two shift stages, if a mid temperature shift catalyst can be found that brings down the CO content to ≤1 vol.%, it will help reduce the size of the fuel processor further. To address this problem, we have taken up a study to prepare Cu-based catalysts supported on various ceria-based mixed oxides that should work at high space velocities.

It was reported that ceria (CeO_2) is an active ingredient for obtaining better water gas shift catalysts due to its ability to undergo rapid reduction/oxidation cycles. The high activity of ceria in redox reactions can be related to its ability to exist in different oxidation states (+3 and +4), the ease with which the oxidation states are changed, its high oxygen storage capacity (OSC) and reducibility [13–16]. As a result of this versatility, CeO_2 is ideal to be used as a support for transition metal catalysts [17–19]. Indeed, CuO supported on ceria is a well-studied system for CO and methane oxidations, and for preferential oxidation of CO in presence of hydrogen [20–22]. However, ceria is prone to sintering under reaction conditions. Whereas, doping with stable cations such as Zr^{4+} was reported to enhance the structural stability of ceria towards sintering [23,24].

The present study deals with the synthesis, characterization and WGS activity of copper on ceria, ceria-zirconia and ceria-titania supports. It attempts to rationalize their catalytic behaviour based on structure–property correlations.

2. Experimental

2.1. Catalyst preparation

Three copper-based mixed oxides, CuO-CeO_2, CuO-CeO_2-ZrO_2 and CuO-CeO_2-TiO_2 were prepared by co-precipitation using dilute solutions to yield high surface area oxides. Appropriate quantities of 0.1 M aqueous solutions of Cu $(NO_3)_2{\cdot}6H_2O$, $Ce(NO_3)_3{\cdot}6H_2O$, $ZrO(NO_3)_2$/$K_2TiO(C_2O_4)_2{\cdot}2H_2O$ were stirred in a round bottom flask and to this solution, KOH was added dropwise to precipitate the corresponding hydroxides. During the precipitation, it was heated at 80 °C under constant stirring while maintaining the pH of the precipitate in 9.5–10 range. Followed by this, the precipitate was aged for 12 h, filtered and washed with distilled water till the pH reached 7.5. The precipitate was dried in an oven at 100 °C for 12 h, crushed and calcined in air in a muffle furnace at 500 °C for 4 h.

2.2. Catalyst characterization

The BET surface area (S_{BET}), of the mixed oxide samples was measured by nitrogen sorption at −196 °C using a NOVA-1200 adsorption unit. The catalyst samples were evacuated at 300 °C for 3 h before measuring N_2 adsorption isotherms. The isotherms were analyzed in a conventional manner in the region of the relative pressure, p/p_0 = 0.05–0.3. Powder X-ray diffraction patterns were collected on a PANalytical X'pert Pro duel goniometer diffractometer equipped with an X'celerator solid-state detector. Nickel filtered Cu Kα (1.5418 Å) radiation was used and the data collection was carried out using a flat holder in Bragg-Brentano geometry (10–90°; 0.2°/min). The mean crystallite sizes of the oxides were calculated by applying Debye–Scherrer equation using the FWHM values of the most intense peaks. Unit cell parameters and crystallite sizes were calculated using X'pert suite of programs.

Diffuse reflectance UV–vis spectra were recorded in the 200–800 nm range at room temperature in reflectance mode using a PerkinElmer spectrometer. The reflectance spectra were converted into the Kubelka-Munk function, $F(R)$ that is proportional to the absorption coefficient for low values of $F(R)$. Temperature programmed reduction (TPR) profiles were obtained using Micromeritics Autochem 2910 catalyst characterization system, equipped with a TCD detector. Freshly calcined samples were pretreated in high purity (99.98%) argon (Ar, 20 ml/min) at 500 °C for 2 h. Followed by cooling to ambient temperature, Ar gas flow was replaced with 5% H_2 in Ar and the catalyst was heated to 800 °C at a heating rate of 10 °C/min. The flow rate of H_2/Ar mixture was kept at 30 ml/min for all the studies. The water produced during the reduction step was condensed and collected in a cold trap immersed in slurry of iso-propanol and liquid nitrogen. X-ray photoemission spectra (XPS) were acquired on a VG Microtech Multilab ESCA 3000 spectrometer using a non-monochromatized Mg Kα (1253.6 eV) and Al Kα (1486.6 eV) X-ray sources.

2.3. Evaluation of catalytic activity

Evaluation of catalytic activity was carried out in a down flow, fixed bed SS316 reactor with 11 mm i.d. (BTRS Jr, Autoclave engineers). All the catalytic tests were carried out at atmospheric pressure in the temperature range of 150–400 °C. About 0.5 cm^3 of the catalyst in the particle size range of 35–50 mesh was loaded in to the tubular reactor that has a thermo well placed in the center of the catalyst bed. The temperature of the catalyst bed is continuously monitored with the help of a Cr-Al thermocouple. All the catalysts were activated in the flow of dry air at 400 °C followed by cooling to the reaction temperature in nitrogen atmosphere. The catalyst was reduced in 20 vol.% H_2 in N_2 gas mixture while raising the temperature from 50 to 200 °C with a ramp rate of 3 °C/min. Two synthetic feed gas mixtures, one without CO_2 (40% H_2 + 10% CO + 50% N_2) and the other containing CO_2 (40% H_2 + 10% CO + 15% CO_2 + 35% N_2) was passed using a thermal mass flow controller at a specified flow rate (GHSV = 5000–25,000 h^{-1}), along with the required amount of H_2O (40% by volume). The water was charged by a high-pressure Isco syringe pump 500D. The product gas mixture was cooled using a chilled water condenser and the dry gas mixture was analyzed online using a Chemito-1000 GC equipped with TCD detector and a Spherocarb packed column (1/8 in. diameter, 8 ft length) that gives base line separation of various gas components present in the stream. A calibrated gas mixture of known composition was used for quantification.

3. Results and discussion

Copper supported on CeO_2 is reported to be highly active for low temperature CO oxidation. Recently, this system has been exploited for WGS reaction [25,26]. The physical and chemical state of the copper species plays an important role here. A recent study revealed that active metal with partial ionic character present in the interface of nano particles and the support influence the activity of the catalyst [27–29]. The effect of particle size of the active metals on catalytic activity is also well studied. Higher loading of CuO on oxide supports can lead to bigger particles and hence lowering of the activity. Moreover, pyrophoricity also increases with copper loading. Hence, we have chosen an optimum loading of 10 wt.% for the current study. Usually, impregnation methods are employed for metal loading on the surface of the supports. However, to facilitate possible stabilization of Cu in ionic form, we have resorted to co-precipitation method which would lead to composite oxides. In this method, a simultaneous precipitation of component hydroxides in the precursor may aid in the surface incorporation of $Cu^{\delta+}$ ions. Hence, 10% CuO-CeO_2 was prepared by co-precipitation method. To study the effects of doping, 10% CuO-CeO_2-ZrO_2 and 10% CuO-CeO_2-TiO_2 were synthesized by the same method. These samples will be referred to as CuCe, CuCeZr and CuCeTi hereafter. For comparison, pure ceria was also prepared following the same procedure as used for

Table 1
Physico-chemical characteristics of the catalysts before and after WGS reaction

Catalyst composition	S_{BET} (m^2/g)		Crystallite size (nm)	
	Fresh	Spent	Fresh	Spent
10% CuO + 90% CeO_2	104	87	7.3	7.4
10% CuO + 45% CeO_2 + 45% ZrO_2	171	97	4.2	4.6
10% CuO + 45% CeO_2 + 45% TiO_2	139	63	3.0	3.0

the other materials. Phase analysis and crystallite size estimation were carried out by powder X-ray diffraction and the results are given in Table 1 and the patterns are shown in Fig. 1.

The XRD pattern of pure ceria showed that it corresponds to the fluorite structure (JCPDS 34-0394). The pattern could be indexed based on the reported data as belonging to cubic system with $a = 5.4118$ Å (Fm-$3m$). Incorporation of Cu did not affect the structure significantly and could be indexed with cell parameter, $a = 5.40$ Å. However, copper is present as CuO as shown by the discernible peaks in the 2θ range 34–42°. The crystallite size of this CuO phase could be calculated using Debye–Scherrer equation to be >20 nm. However, the overall surface area is high and the ceria particle size was around 8 nm. This shows that the CuO phase exists outside the bulk ceria as big crystallites. However, in the zirconia and titania doped systems, CuO peaks were absent which is expected for low metal loading which in turn leads to very small crystallites highly dispersed in the support matrix. This also points to a possible size of <3 nm for the CuO particles. The small size of CuO clusters can promote more interactions with the support and hence enhance $Cu^{\delta+}$ ions in the metal–support interface during reduction. The cell parameter of the fluorite ceria was affected by doping with zirconia and titania ($a = 5.32$ Å) indicating the formation of a solid solution. This is further corroborated by the absence of any individual zirconia or titania phase peaks. Moreover, the crystallinity of the ceria phase decreased by doping with zirconia; the effect being more pronounced with titania. It is quite possible that at the percentage substitution used in this study, zirconia leads to better structural stability than titania.

The chemical state in which the copper oxide phase exists in all the three catalysts was followed by X-ray photoelectron spectroscopy and UV–vis spectroscopy. The results showed the presence

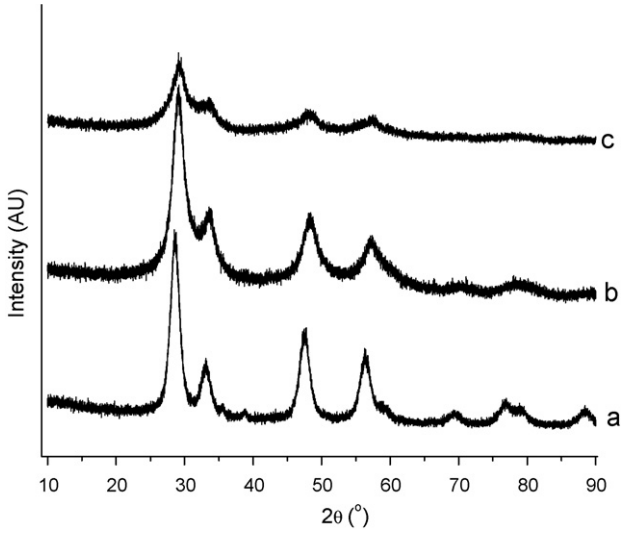

Fig. 1. XRD patterns of fresh (a) CuO-CeO_2; (b) CuO-CeO_2-ZrO_2; (c) CuO-CeO_2-TiO_2 samples.

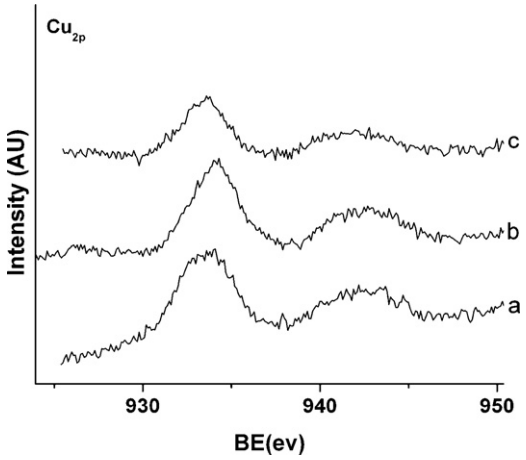

Fig. 2. Cu 2p core level XPS spectra of (a) CuO-CeO_2; (b) CuO-CeO_2-ZrO_2; (c) CuO-CeO_2-TiO_2 samples.

of Cu^{2+} [30] as evident from the main peak in the 934.0–933.7 eV range (Fig. 2). The satellite peaks point to the presence of d^9 configuration as in Cu^{2+}. Presence of reduced copper species is usually manifested in the intensity ratios of the main peaks and the satellite peaks. In the above compounds, the area under the satellite peaks was found to be ≥0.55 indicating that the copper exists as Cu^{2+}. The Ce 3d region of CuCe showed a typical CeO_2 spectrum with two main peaks at 916.7 and 882 eV with the corresponding satellites. However, doping with ZrO_2 and TiO_2 seems to lead to a much broader spectrum with reduced satellite peak intensities. There is no evidence of the presence of Ce in lower oxidation states.

UV–vis spectra (Fig. 3) show the presence of broad peaks in the region of 210–270 nm corresponding to the charge transfer bands. This band indicates the $O_2 \rightarrow Cu^{2+}$ ligand to metal charge transfer (LMCT) transition [31]. The interesting factor here is the intensity variation between the samples. The LMCT band corresponding to CuCeZr was found to be more intense than the other two samples. This might indicate a better interaction of Cu^{2+} species with the oxide support in case of CuCeZr.

The physical properties of the catalysts like reducibility, metal–support interactions, etc. are found to have profound effect on their WGS activity. The WGS activity tests on these catalysts show that this indeed is the case. We found discernible differences in the behaviour of CuCeTi and the other two copper catalysts. First the CO conversion was followed in the absence of CO_2 (Fig. 4). The CuCe

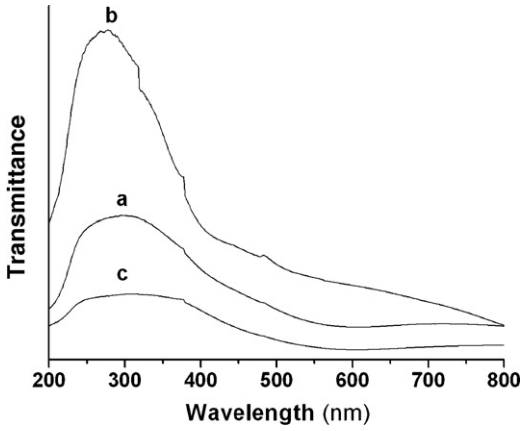

Fig. 3. UV–vis spectra of (a) CuO-CeO_2; (b) CuO-CeO_2-ZrO_2; (c) CuO-CeO_2-TiO_2.

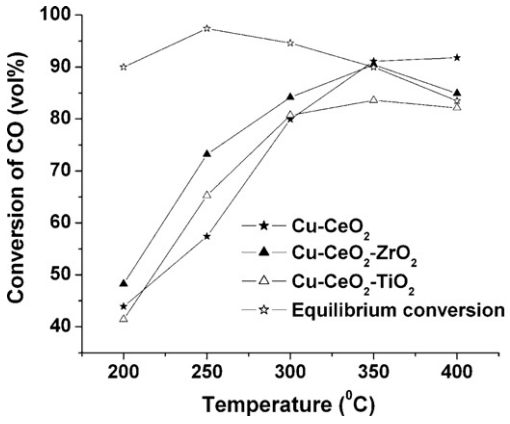

Fig. 4. CO conversion in the absence of CO_2 in the feed gas mixture. (☆) Equilibrium conversion; (★) CuO-CeO_2; (▲) CuO-CeO_2-ZrO_2; (△) CuO-CeO_2-TiO_2.

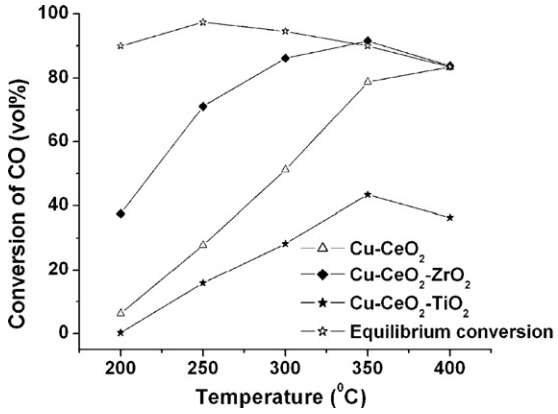

Fig. 5. CO conversion in presence of CO_2 in the feed gas mixture. (☆) Equilibrium conversion; (△) CuO-CeO_2; (◆) CuO-CeO_2-ZrO_2; (★) CuO-CeO_2-TiO_2.

and CuCeZr catalysts achieved the theoretical equilibrium conversion at 350 °C reaching a conversion of 90%. Whereas, on CuCeTi catalyst, the maximum CO conversion that could be attained was only 83% at 350 °C. However, in real conditions, the CO_2 co-existing in the reformed gas greatly influences the CO conversion in the water gas shift reaction. As water gas shift is a reversible reaction, the CO_2 in the gas mixture should influence the CO conversion to a large extent. Hence, activity tests were carried out under equilibrium conditions under which the differences between

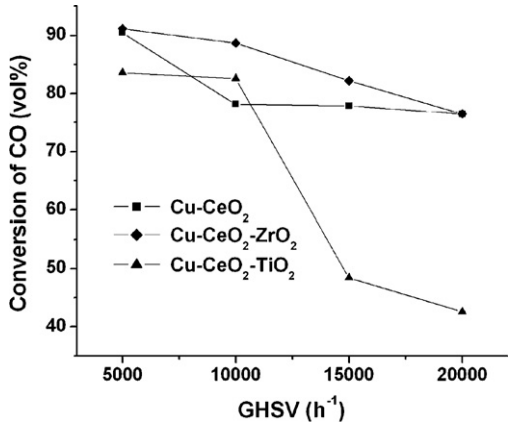

Fig. 6. CO conversion as a function of space velocity in the absence of CO_2 in feed. (■) CuO-CeO_2; (◆) CuO-CeO_2-ZrO_2; (▲) CuO-CeO_2-TiO_2.

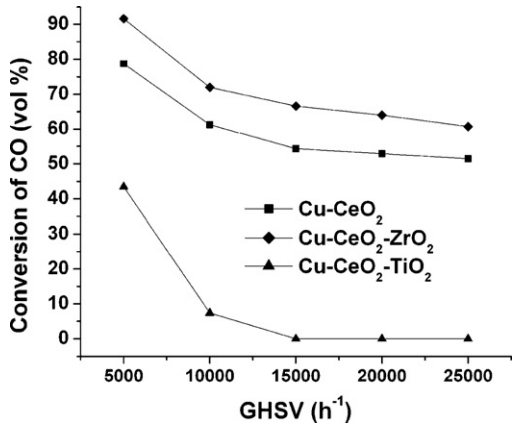

Fig. 7. CO conversion as a function of space velocity with CO_2 containing feed. (■) CuO-CeO_2; (◆) CuO-CeO_2-ZrO_2; (▲) CuO-CeO_2-TiO_2.

CuCeZr and the other two catalysts becoming more pronounced. Fig. 5 shows the effect of CO_2 in the feed gas. The CO conversion decreases to 43 and 78% respectively in case of CuCeTi and CuCe, these values are far away from equilibrium conversions. However, the CuCeZr catalyst still gives equilibrium conversion of CO at 350 °C. A similar effect is also seen when space velocity is increased. Figs. 6 and 7 show the effect of space velocity on WGS activity at 350 °C in the absence and presence of CO_2 in the feed gas mixture respectively. The tests were performed at space velocities varying between 5000 and 25,000 h^{-1}. The CuCe and CuCeZr show reasonably good CO conversion even at higher space velocities and the conversion falls gradually as the space velocity is increased. But, in the case of CuO-CeO_2-TiO_2 catalyst, the CO conversion decreased very rapidly as the space velocity is increased. The fact that the activity was affected by the introduction of CO_2 thereby affecting the equilibrium prompted us to study the reverse water gas shift (RWGS) activity of the TiO_2 doped catalyst. This reaction was carried out with equilibrium concentrations of H_2 and CO_2. Interestingly, the catalyst did not exhibit any RWGS activity.

As mentioned earlier, the differences in WGS activity exhibited by catalysts based on different supports can only be attributed to the effect of the doping oxides on the catalyst characteristics like reducibility of copper species. This was studied by TPR measurements. Each Cu-based sample showed characteristic behaviour as shown in Fig. 8. TPR studies were carried out in the temperature range 50–900 °C. In the case of CuCe catalyst, two reduction peaks were seen at 150 and 184 °C. These can be attributed to the

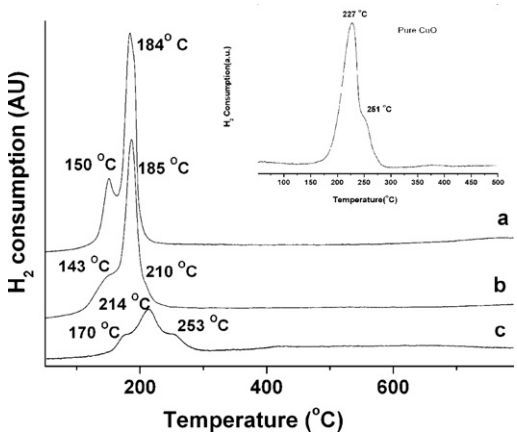

Fig. 8. TPR profiles of (a) CuO-CeO_2, (b) CuO-CeO_2-ZrO_2 and (c) CuO-CeO_2-TiO_2 (inset, TPR profile of pure CuO).

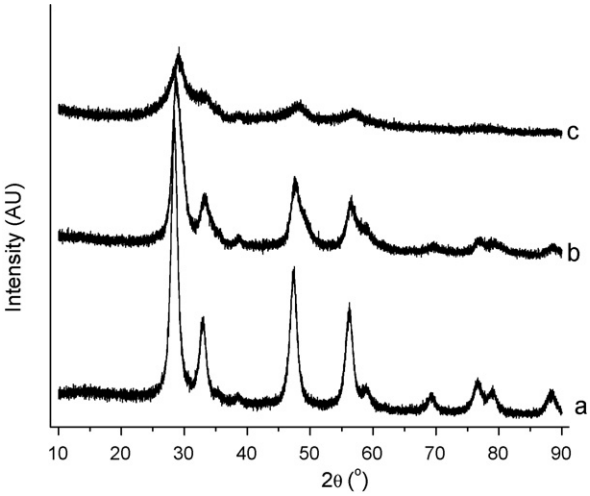

Fig. 9. XRD patterns of spent catalysts (a) CuO-CeO_2; (b) CuO-CeO_2-ZrO_2; (c) CuO-CeO_2-TiO_2.

reduction of highly dispersed copper in close interaction with CeO_2 matrix and the bulk like copper oxide or its clusters which are relatively difficult to reduce, respectively [32]. Though CuO may be reduced in two steps, $Cu^{2+} \rightarrow Cu^{1+}$ and $Cu^{1+} \rightarrow Cu^0$, literature reports suggest that Cu^{2+} is reduced in a single step. The hydrogen consumption of HT peak was several times higher than that of LT peak indicating that the latter reduction step consumes more hydrogen, as it may have contribution from reduction of CeO_2, along with Cu^{2+} reduction, as a result of spillover effect [21,27,33,34]. When compared to the profile of crystalline CuO, the reduction peaks are shifted much to lower temperatures. This is due to the effect of the support on the reducibility of CuO and also the presence of well-dispersed Cu^{2+} ions [35]. However, in the case of CuCeZr, the reduction starts at slightly lower temperature (143 °C) evidencing an enhanced reducibility with the addition of ZrO_2. Interestingly, in the case of CuCeTi, the profile was very different from that of other two catalysts, showing three reduction peaks. Moreover, overall reduction temperatures also increased by more than 20 °C. Hence unlike ZrO_2, addition of TiO_2 to CeO_2 seems to have a negative effect on the overall reducibility of the catalyst.

The catalytic behaviour can also be better understood by characterization of the spent catalysts. As given in Table 1, the surface areas of all the three catalysts were reduced after the WGS reaction. Contrary to the expectations, the doped oxides underwent more sintering. However, this effect is not very pronounced in crystallite sizes which remained more or less same after the reaction. The reaction condition under which WGS is carried out is highly reducing. Hence, a reduction of the CuO phase to metallic Cu *in situ* is expected, in spite of water being present in the stream. However, Cu being highly pyrophoric, on exposure to air, Cu metallic phase is completely oxidized back to the CuO phase. Instead of a direct observation of metallic Cu, we focused on the CuO phase before and after WGS reaction. The ~20 nm CuO particles in CuCe catalyst, after WGS reaction, became much more dispersed (Fig. 9). Hence we can envisage the formation of highly dispersed active metallic Cu under the reducing ambience of the reaction. The CuCeZr and CuCeTi catalysts, however, showed an opposite behaviour. The CuO particles were very small (<3 nm) and highly dispersed in the oxide matrix to begin with and after the reaction, the phase could be clearly seen in XRD spectra. In the case of CuCeZr, the particle size of the re-oxidized CuO is more than that in CuCeTi; both are albeit highly dispersed. Hence, it is quite possible that the active sites in all the three catalysts have more or less the same physical characteristics during the reaction.

4. Conclusions

The activity of Cu-based catalysts with different supports has been investigated using synthetic gas mixture that mimics the realistic conditions of WGS reaction. Among the catalysts reported, CuO-CeO_2-ZrO_2 and CuO-CeO_2 composites showed better performance when compared to CuO-CeO_2-TiO_2. Even though doping is expected to increase the stability, in case of TiO_2 doping, it was observed from XRD studies, that the crystallinity of CuO-CeO_2-TiO_2 is not enhanced; on the contrary, it had an adverse effect. However, presence of CuO phase of similar characteristics in the spent catalysts indicates that it is possible that the active copper metallic phases in all the catalysts were also similar during the reaction. The observed differences between the catalytic behaviour, hence, could only be attributed to the difference in interaction of CuO phase with the different supports used. As evidenced from TPR studies, reducibility may play an important role in enhancing the activity.

References

[1] P.G. Patil, J. Power Sources 37 (1992) 171.
[2] J.C. Amphlett, R.M. Baumert, R.F. Mann, B.A. Peppley, P.R. Roberge, T.J. Harris, J. Electrochem. Soc. 142 (1995) 1.
[3] T. Isono, S. Suzuki, M. Kaneko, Y. Akiyama, Y. Miyaki, I. Yonezu, J. Power Sources 86 (2000) 269.
[4] S. Kawatsu, J. Power Sources 71 (1998) 150.
[5] J.R. Ladebeck, J.P. Wagner, in: W. Vielstich, et al. (Eds.), Handbook of Fuel Cell Technology—Fundamentals, Technology and Applications, Wiley, 2003 (Chapter 7).
[6] M.A. Rosen, D.S. Scott, Int. J. Hydrogen Energy 23 (1998) 653.
[7] A.F. Ghenciu, Curr. Opin. Solid State Mater. Sci. 6 (2002) 389.
[8] D.L. Trimm, Appl. Catal. A: Gen. 296 (2005) 1.
[9] D.S. Newsome, Catal. Rev. Sci. Eng. 21 (1980) 275.
[10] C. Rhodes, G.J. Hutchings, A.M. Ward, Catal. Today 23 (1995) 43.
[11] R.L. Keiski, T. Salmi, P. Niemisto, J. Ainassaari, V.J. Pohjola, Appl. Catal. A: Gen. 137 (1996) 349.
[12] T. Giroux, S. Hwang, Y. Liu, W. Ruettinger, L. Shore, Appl. Catal. B: Environ. 56 (2005) 95.
[13] X. Wang, J.A. Rodriguez, J.C. Hanson, D. Gamarra, A. Martinez Arias, M.F. Garcia, J. Phys. Chem. B 110 (2006) 428.
[14] Q. Liu, Q. Zhang, W. Ma, R. He, L. Kou, Z. Mou, Prog. Chem. 17 (2005) 389.
[15] C. Padeste, N.W. Cant, D.L. Trimm, Catal. Lett. 18 (1993) 305.
[16] G.S. Zafiris, R.J. Gorte, J. Catal. 139 (1993) 561.
[17] T. Bunluesin, R.J. Gorte, G.W. Graham, Appl. Catal. B: Environ. 15 (1998) 107.
[18] S. Hilaire, X. Wang, T. Luo, R.J. Gorte, J. Wagner, Appl. Catal. A: Gen. 215 (2001) 271.
[19] X. Liu, W. Ruettinger, X. Xu, R. Farrauto, Appl. Catal. B: Environ. 56 (2005) 69.
[20] M. Ronning, F. Huber, H. Meland, H. Venvik, D. Chen, A. Holmen, Catal. Today 100 (2005) 249.
[21] W. Liu, M. Flytzani-Stephanopoulos, J. Catal. 153 (1995) 304.
[22] W. Liu, M. Flytzani-Stephanopoulos, J. Catal. 153 (1995) 317.
[23] T. Sato, K. Dosaka, H. Ishitsuka, E.M. Haga, A. Okuwaki, J. Alloys Compd. 193 (1993) 274.
[24] E. Tani, M. Yoshimura, S. Somiya, J. Am. Ceram. Soc. 66 (1983) 506.
[25] N.A. Koryabkina, A.A. Phatak, W.F. Ruettinger, R.J. Farrauto, F.H. Ribeiro, J. Catal. 217 (2003) 233.
[26] Y. Tanaka, T. Utaka, R. Kikuchi, K. Sasaki, K. Eguchi, Appl. Catal. A: Gen. 242 (2003) 287.
[27] Q. Fu, S. Kudriavtseva, H. Saltsburg, M. Flytzani-Stephanopoulos, Chem. Eng. J. 93 (2003) 41.
[28] Q. Fu, H. Satlsburg, M. Flytzani-Stephanopoulos, Science 301 (2003) 935.
[29] X. Qi, M. Flytzani-Stephanopoulos, Ind. Eng. Chem. Res. 43 (2004) 3055.
[30] C.-K. Wu, M. Yin, S. O'Brien, J.T. Koberstein, Chem. Mater. 18 (2006) 6054.
[31] H. Praliaud, S. Mikhailenko, Z. Chajar, M. Primet, Appl. Catal. B: Environ. 16 (1998) 359.
[32] M.-F. Luo, Y.-J. Zhong, X.-X. Yuan, X.-M. Zheng, Appl. Catal. A: Gen. 162 (1997) 121.
[33] W. Liu, M. Flytzani-Stephanopoulos, Chem. Eng. J. 64 (1996) 283.
[34] Y. Li, Q. Fu, M. Flytzani-Stephanopoulos, Appl. Catal. B: Environ. 27 (2000) 179.
[35] C.R. Jung, J. Han, S.W. Nam, T.-H. Lim, S.-A. Hong, H.-I. Lee, Catal. Today 93–95 (2004) 183.